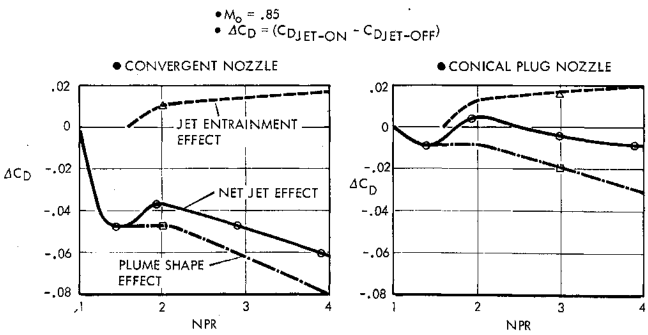

Fig. 14 General trends of jet effects.

ratios for which they are designed. This is due to their inability to simulate jet entrainment effects.

V. Conclusions

The following conclusions are made for the configurations tested.

1) Flow entrainment caused by the exhaust jet affects boattail flow significantly. This may, in part, explain why experimenters have had only varying success in duplicating jet effects with solid, plume-shaped extensions. Solid extensions may adequately simulate exhaust jets which entrain relatively little external flow as, for example, can be the case in ejector-type nozzles.[2] Since an ejector nozzle pumps internal secondary flow, its ability to entrain boattail flow is diminished. However, as seen in the General Dynamics tests, jet entrainment of the nonejector nozzles tested readily affects boattail flow whereas solid extensions do not reproduce this effect.

2) The boattail tested has three to four times more drag with conical plug exhaust flow than with axially directed convergent flow. This illustrates the strong effect of plume shape on boattail flowfield.

3) Drag levels on the typical force-model nozzle are misleading. The flow-through-nacelle nozzle tested exhibits different drag levels than do counterpart engine nozzles. This result is explained by particular differences in plume shape and entrainment effects.

References

[1] Shrewsbury, G. D., "Effect of Boattail Juncture Shape on Pressure Drag Coefficients of Isolated Afterbodies," TM X-1517, March 1968, NASA.

[2] Harrington, D. E., "Jet Effects on Boattail Pressure Drag of Isolated Ejector Nozzles at Mach Numbers from 0.60 to 1.47," TM X-1785, May 1969, NASA.

JUNE 1971 J. AIRCRAFT VOL. 8, NO. 6

Combined Inertial—ILS Aircraft Navigation Systems

JAMES W. BURROWS*
The Boeing Company, Seattle, Wash.

Error models for the Instrument Landing System (ILS) and Inertial Navigation System (INS) are discussed. A method for combining the two systems using the theory of optimal linear estimation is given. Results of tests of the combined navigation system using a ground vehicle operating on runways and instrumented with an inertial navigator, radio receivers, and a computer, are given with emphasis on the effects of initialization and unmodeled errors. The results indicate that use of the combined system during landing approach would simultaneously reduce the cross-runway position and velocity (track angle) errors. The combined system is relatively insensitive to the choice of initial values of certain parameters. Results are still good when the initial parameter values are chosen to approximate a real-time least square fit of INS position and velocity to the ILS localizer signal. The effects of the principal unmodeled error, platform tilt, are such that the tilt would have to be precorrected or included in the error model during approach if a poorer INS were to be employed.

Instrument Landing System (ILS) and Its Errors

SINCE its development just before World War II, the ILS has become the principal method of aircraft navigation during final approach to a landing at larger airports in bad weather. As of the beginning of 1969, there were 377 ILS installations in the United States, and probably that many again in the rest of the world. The principal component of the system is the localizer, which provides lateral course information. It consists of two directional antennas whose patterns are symmetrically placed with respect to the runway centerline. The carrier from one is modulated with a 90-Hz tone, and the other with 150 Hz. The aircraft localizer receiver compares the output of two audio filters centered on the modulation frequencies. The output of the receiver should be proportional to the angle from the aircraft to the runway centerline at the localizer antenna. Additional components of the ILS are the glide slope for descent information, marker beacons and compass locators for range information, and last, but not least, approach lights.[1]

The output of the localizer receiver usually varies from the above proportionality relationship. It has long been recognized that these errors are due to radiation scattering from objects illuminated by the localizer transmitter.[2] Indeed, a plot of the localizer receiver output along the runway

Received October 8, 1969; revision received February 24, 1970. The author wishes to thank the staff of the Automatic Flight Management Laboratory of The Boeing Commercial Airplane Division for their devoted labor during the tests reported in this paper, particularly G. Hadley, who programed most of the real time and post-run computations.

* Senior Specialist Engineer, Mathematical Sciences, Aerospace Group.

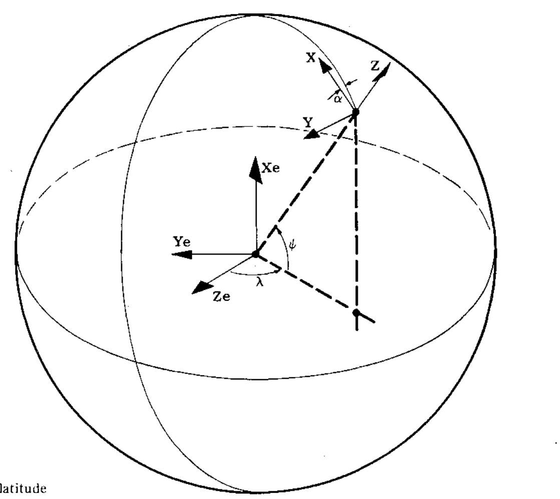

ψ = latitude

λ = longitude

α = wander angle

C: earth fixed $(x_e, y_e, z_e) \rightarrow$ platform(x,y,z).

$$C = \begin{pmatrix} \cos\alpha\cos\psi & \sin\alpha\cos\lambda + \cos\alpha\sin\lambda\sin\psi & \sin\alpha\sin\lambda - \cos\alpha\cos\lambda\sin\psi \\ -\sin\alpha\cos\psi & \cos\alpha\cos\lambda - \sin\alpha\sin\lambda\sin\psi & \cos\alpha\sin\lambda + \sin\alpha\cos\lambda\sin\psi \\ \sin\psi & -\sin\lambda\cos\psi & \cos\lambda\cos\psi \end{pmatrix}$$

Fig. 1 INS coordinate systems.

centerline may be regarded as a one-dimensional hologram at the localizer frequency of the scattering objects. Some proposals have been made that the scattering objects could be identified using optical correlation techniques and some nonreflecting coating applied. This proposal is not a very good cure for the localizer transients caused by taxiing or low-flying aircraft.

Plots of the output of a localizer receiver along the runway centerline extension of runways at several U.S. airports are given in Ref. 3. Actual aircraft excursions from the centerline were corrected by theodolite tracking. Analog simulations of approaches with various damping schemes for the localizer coupler using those inputs resulted in errors as large as 40 m and 3.2 m/sec (the standard half-runway width is about 22.5 m or 75 ft).[3]

Inertial Navigation System (INS) and Its Errors

The development of inertial navigation began with the marine gyrocompass in the early 1900's. For aircraft an INS comprises a gimbaled platform on which accelerometers and gyroscopes are mounted, and a computer for integrating the accelerometer outputs, computing the acceleration due to gravity, and controlling the attitude of the platform.[4] For accelerometer accuracy reasons, the computation of gravity is avoided by keeping two of the accelerometers orthogonal to the Earth's gravity field; this is known as a locally level mechanization. If one of the level accelerometers is held in a north-south direction, the mechanization is further characterized as north-pointing, if not, a wander angle mechanization.

Figure 1 gives the orthogonal matrix C for the rotation from the Earth fixed coordinate system x_e,y_e,z_e to a system parallel to the platform coordinate system x,y,z for an INS with a typical locally level wander angle mechanization. The navigation equations for such an INS may be written

$$\dot{C} = \begin{pmatrix} 0 & 0 & -\omega_y \\ 0 & 0 & \omega_x \\ \omega_y & -\omega_x & 0 \end{pmatrix} C \tag{1}$$

$$\dot{v}_x = a_x + 2\Omega c_{31} v_y, \qquad \dot{v}_y = a_y - 2\Omega c_{31} v_x \tag{2}$$

$$\omega_x = -v_y(1 - fc_{31}^2 + 2fc_{11}^2 - h/a)/a - 2fv_x c_{11} c_{21}/a \tag{3a}$$

$$\omega_y = v_x(1 - fc_{31}^2 + 2fc_{21}^2 - h/a)/a + 2fv_y c_{11} c_{21}/a \tag{3b}$$

Equations (1) and (2) are really the double integrations of the level accelerometer outputs a_x,a_y, first finding the platform velocities v_x,v_y, then the orthogonal matrix C. The additional terms of Eq. (2) are corrections for Coriolis acceleration due to rotation of the Earth fixed coordinate system at Ω = 15.041 deg/hr. ω_x,ω_y are the platform rates with respect to the Earth required to keep the platform locally level at an (assumed constant) height h above the oblate Earth with ellipticity f = 1/297.0, equatorial radius a = 6378 km. The gyroscopes are precessed so that the platform angular rates with respect to inertial space are

$$T_x = \omega_x + \Omega c_{11}, \qquad T_y = \omega_y + \Omega c_{21} \tag{4a}$$

$$T_z = \Omega c_{31} \tag{4b}$$

to keep the platform physically locally level. From Eq. (4b), the azimuth of a platform axis "wanders" when the platform is moved in longitude, hence the name of the mechanization. The current values of latitude, longitude, and wander angle are obtainable from the C matrix.

After having moved over the Earth's surface and arrived at a certain point, let the correct value of the rotation matrix be C. The computer will say the value of the rotation matrix is C_c, and let the value of the matrix of the rotation from Earth fixed to the actual platform coordinate system be C_p. Assume that the orthogonal transformation from C to C_c may be approximated by the infinitesimal rotation $\boldsymbol{\delta\theta}$, then by taking differentials of Eq. (1), (cf. Fig. 2)

$$\boldsymbol{\delta\theta} + \boldsymbol{\omega} \times \boldsymbol{\delta\theta} = \boldsymbol{\delta\omega} \tag{5}$$

where, from Eq. (3), $\boldsymbol{\delta\omega}$, the error in the angular rate $\boldsymbol{\omega} = (\omega_x,\omega_y,0)$ is

$$\delta\omega_x = -\delta v_y/a, \qquad \delta\omega_y = \delta v_x/a \tag{6}$$

to first order in ellipticity and errors, $\delta v_x,\delta v_y$ being velocity errors. From the definition of the matrix C, $\delta\theta_x$ and $\delta\theta_y$ are related to the position errors of the INS, in fact,

$$\delta x = a\delta\theta_y, \qquad \delta y = -a\delta\theta_x \tag{7}$$

are the position errors in the platform x and y directions. $\delta\theta_z$ will be called the computer azimuth error.

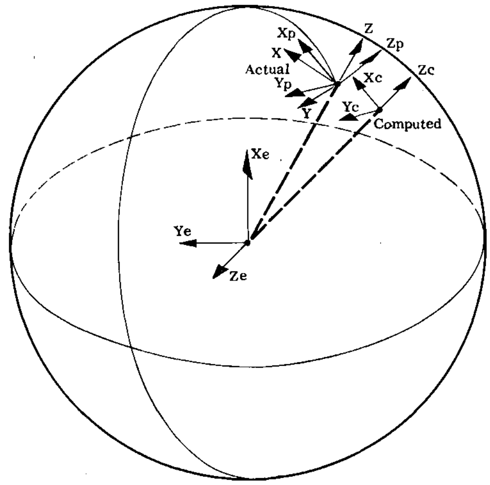

C: earth fixed $(x_e,y_e,z_e) \rightarrow$ correct platform (x,y,z)

C_p: $(x_e,y_e,z_e) \rightarrow$ actual platform (x_p,y_p,z_p); $C_p \doteq (I + [\Phi])C$

C_c: $(x_e,y_e,z_e) \rightarrow$ computed platform (x_c,y_c,z_c); $C_c \doteq (I + [\delta\theta])C$

Fig. 2 INS errors.

Similarly, the (assumed) infinitesimal rotation $\boldsymbol{\varphi}$ from C to Cp solves the differential equation

$$\dot{\boldsymbol{\varphi}} + (\boldsymbol{\Omega} + \boldsymbol{\omega}) \times \boldsymbol{\varphi} = \boldsymbol{\delta\Omega} + \boldsymbol{\delta\omega} + \boldsymbol{\varepsilon} \tag{8}$$

where $\boldsymbol{\delta\Omega}$ is the error vector $\Omega(\delta c_{11},\delta c_{21},\delta c_{31})$, which may be approximated using C_c and $\boldsymbol{\delta\theta}$, and $\boldsymbol{\varepsilon}$ is the gyro drift vector. φ_x and φ_y are called the platform tilts, since they are the angular amounts by which the platform is off from locally level; φ_z is the platform azimuth error. Finally, by taking differentials in the equation from which Eq. (2) is derived, the error in the velocities

$$\boldsymbol{\delta\dot{v}} = \boldsymbol{\delta v} \times (2\boldsymbol{\Omega} + \boldsymbol{\omega}) + \mathbf{v} \times (2\boldsymbol{\delta\Omega} + \boldsymbol{\delta\omega}) + \mathbf{a}_s \times \boldsymbol{\varphi} + 2g\delta z\mathbf{k}/a + \mathbf{b} \tag{9}$$

where $\mathbf{a}_s$ is the sensed acceleration [in level flight $\mathbf{a}_s = (a_x,a_y,g)$] and $\mathbf{b}$ is the vector of accelerometer errors.

A multitude of mechanical shortcomings are lumped into the instrument error vectors $\boldsymbol{\varepsilon}$ and $\mathbf{b}$. For example, gyro bias errors, mass unbalance drift, anisoelastic drift, scale factor error, and input axis misalignments; accelerometer bias error, scale factor error, and input axis misalignments. Instruments in use today for commercial INS are generally capable of sustained and repeatable performance with $|\boldsymbol{\varepsilon}| < 5 \times 10^{-8}$ rad/sec and $|\mathbf{b}| < 10^{-3}$ m/sec^2. A more easily applied measure of the quality of an INS is its CEP rate in knots, i.e., the terminal radial error in nautical miles divided by the duration of the flight in hours, the median taken over many flights. An INS manufacturer can get in trouble with the Defense Department if it tries to advertise for export trade an INS with performance better than 1 knot, so the prevalent claim is $1 + \epsilon$ knot. This is an over-all figure, not to be confused with the instantaneous velocity error of Eq. (9) which can be on the order of 4–5 m/sec. Similarly, the tilt errors of Eq. (8) are generally smaller than 1 mrad.

For a short period of time (1 hr), the dominant x,y terms of Eqs. (5, 8, and 9) may be written

$$\delta\dot{x} = \delta v_x - v_y\delta\theta_z,\ \delta\dot{y} = \delta v_y + v_x\delta\theta_z,\ \delta\dot{\theta}_z = 0 \tag{10a}$$

$$\delta\dot{v}_x = -g\varphi_y, \qquad \delta\dot{v}_y = g\varphi_x \tag{10b}$$

$$\dot{\varphi}_y = \delta v_x/a, \qquad \dot{\varphi}_x = -\delta v_y/a \tag{10c}$$

The solution to the tilt and velocity error equations in Eq. (10) is an oscillation with the famous Schuler period of $2\pi(a/g)^{1/2}$ or 84.4 min. A tilt amplitude of 1 mrad corresponds to a velocity error amplitude of about 8 m/sec.

Combined ILS-INS

A locally level coordinate system was set up with the origin at the localizer antenna, the x axis down the runway centerline, and the y axis cross runway. An initial position (x_{r0},y_{r0}) and velocity (v_{rx0},v_{ry0}) were chosen in this coordinate system, and subsequent motion as observed by the inertial platform was computed by summing, with Coriolis corrections, the outputs of the integrating accelerometers, rotated through the difference between platform wander angle and runway direction; i.e.,

$$\begin{pmatrix}\Delta v_{rx}\\ \Delta v_{ry}\end{pmatrix} = \begin{pmatrix}\cos(\alpha_r - \alpha) & \sin(\alpha_r - \alpha)\\ -\sin(\alpha_r - \alpha) & \cos(\alpha_r - \alpha)\end{pmatrix}\begin{pmatrix}\Delta v_x\\ \Delta v_y\end{pmatrix} + 2\Omega\Delta t\sin\Psi_r\begin{pmatrix}v_{rx}\\ -v_{ry}\end{pmatrix} \tag{11}$$

is the change in velocity in runway coordinates, where α is the wander angle of the platform and α_r is the runway azimuth; $\Delta v_x,\Delta v_y$ are the accelerometer readouts, in velocity units per frame time Δt of the INS. The last term is the Coriolis correction at latitude Ψ_r. Velocity and position in runway coordinates are then given by

$$\begin{pmatrix}v_{rx}\\ v_{ry}\end{pmatrix} = \begin{pmatrix}v_{rx0}\\ v_{ry0}\end{pmatrix} + \Sigma\begin{pmatrix}\Delta v_{rx}\\ \Delta v_{ry}\end{pmatrix} \tag{12}$$

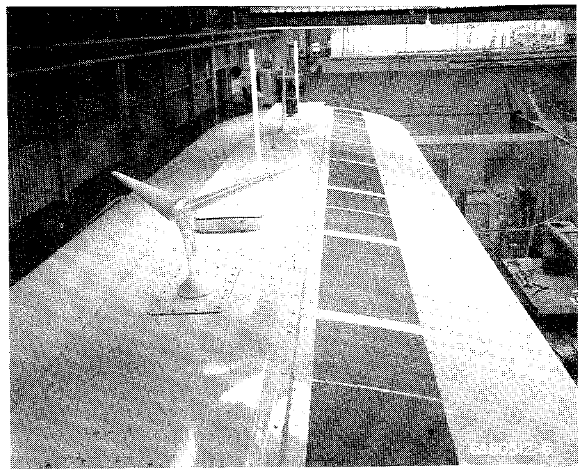

Fig. 3 Test vehicle antenna array.

$$\begin{pmatrix}x_r\\ y_r\end{pmatrix} = \begin{pmatrix}x_{r0}\\ y_{r0}\end{pmatrix} + \Delta t\Sigma\begin{pmatrix}v_{rx}\\ v_{ry}\end{pmatrix} \tag{13}$$

The error equations (10) were further simplified by ignoring the existence of tilt, changing velocities and changing wander angle to give

$$\delta\dot{x}_r = \delta v_{rx}, \qquad \delta\dot{y}_r = \delta v_{ry} \tag{14a}$$

$$\delta\dot{v}_{rx} = 0, \qquad \delta\dot{v}_{ry} = 0 \tag{14b}$$

When solved, these equations give the assumed transition matrix connecting errors at time t_i with those at time t_{i-1}

$$\begin{pmatrix}\delta x_r\\ \delta v_{rx}\\ \delta y_r\\ \delta v_{ry}\end{pmatrix}_i = F_{i-1}\begin{pmatrix}\delta x_r\\ \delta v_{rx}\\ \delta y_r\\ \delta v_{ry}\end{pmatrix}_{i-1} \tag{15}$$

where

$$F_{i-1} = \begin{pmatrix}1 & \tau & 0 & 0\\ 0 & 1 & 0 & 0\\ 0 & 0 & 1 & \tau\\ 0 & 0 & 0 & 1\end{pmatrix} \tag{16}$$

τ being the assumed constant interval between time t_{i-1} and t_i. The difference z_i between the measured localizer reading ϵ_i and the expected reading in microamps was computed every second:

$$z_i = \epsilon_i - K\tan^{-1}(y_r/x_r) \tag{17}$$

where K is a constant associated with the localizer installation, μa/rad. The difference in Eq. (17) is approximately equal to a linear combination of the state variables in Eq. (15) plus noise v_i

$$z_i = H_i(\delta x_r,\delta v_{rx},\delta y_r,\delta v_{ry})_i{}^T + v_i \tag{18}$$

where

$$H_i = [-Ky_r/(x_r{}^2 + y_r{}^2),0,Kx_r/(x_r{}^2 + y_r{}^2),0] \tag{19}$$

A formal application of the Kalman theory (Appendix) gives estimates $(\widehat{\delta x_r},\widehat{\delta v_{rx}},\widehat{\delta y_r},\widehat{\delta v_{ry}})_i$ of the current errors which are to be added to the positions and velocities of Eqs. (12) and (13).

Real Time Tests

Several seats in a SceniCruiser bus were replaced with electronic racks containing a Litton LTN-51 inertial navigator, Bendix RNA-26C radio receiver, Honeywell DDP-124 digital computer, 3 x-y plotters, a magnetic tape recorder and associated power supplies and interface electronics; the antenna array is shown in Fig. 3. The bus was driven down

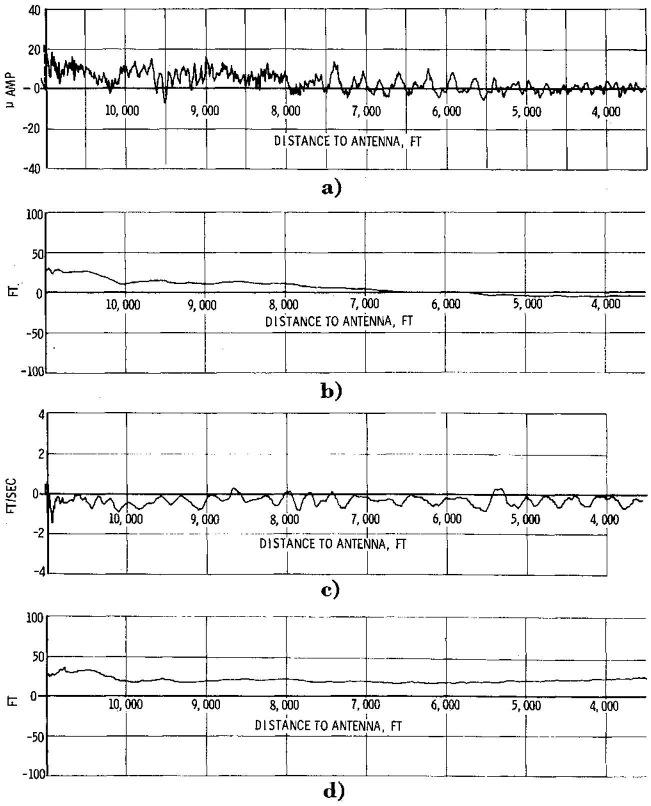

Fig. 4 a) Localizer error; b) cross-runway position error; c) cross-runway velocity error; and d) cross-runway position error (1 mrad tilt), SEA runway 34.

the centerlines of several ILS-equipped runways in the Seattle area at 40–50 mph. While in motion down the runway, the INS accelerometers were read and the "dead reckoning" computations (11–13) performed every 50 msec, the localizer receiver was read, the computations (17), (19), and the required Kalman matrix operations to generate error estimates to be added to the position and velocities were performed every second. The localizer error, the cross-runway position estimate, and the cross-runway velocity estimate (Fig. 4) were plotted on the x-y plotters (the plotter x axes were driven by an independent distance counter mounted on one of the bus wheels). These plots were generated during a run down the centerline of runway 34 at Seattle-Tacoma International Airport.

To interpret these plots as errors of the navigation system requires a knowledge of how accurately the bus was driven down the runway centerline. It was estimated that this was done to within a foot or so, which indicates that Fig. 4b is mostly navigation error, but it is felt that the velocity excursions of Fig. 4c are more steering correction than navigation error.

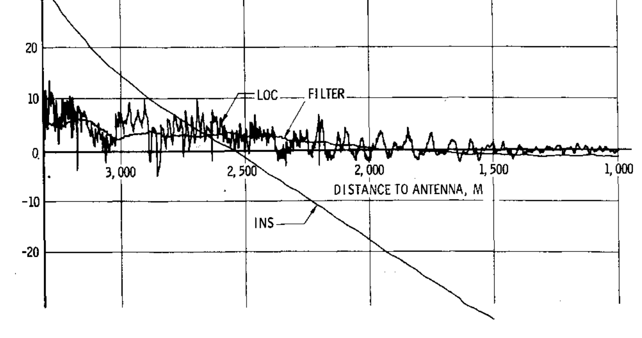

Fig. 5 Cross-runway position error, SEA runway 34, rerun.

To the extent that the localizer error on the runway centerline is representative of that experienced off the centerline, and depending on the accuracy of the knowledge of range to the localizer antenna, these plots, interpreted as errors with the provisos mentioned previously, should be relatively insensitive to the actual path of the observer. Such would not be the case for a non inertially aided localizer filter.

Before the next run, the INS platform was tilted 1 mrad about the down-runway axis, thus giving a nearly constant cross-runway acceleration error of 0.01 m/sec². The resultant position error is shown in Fig. 4d. This indicates that a tilt this large, which would be unlikely in a high quality INS, would either have to be corrected prior to the approach (using VOR-DME information, for example) or reduced during the approach by using Eqs. (10) for the INS error model in place of Eq. (14).

Post-Test Reruns

During the actual run down the runway centerline, the localizer readings and the accelerometer outputs were logged on magnetic tape which made possible post-test reruns with different initializations. Figure 5 shows reruns of the data in Figs. 4a–c. The INS curve is the unaided inertial cross-runway position error when $(\delta y_r)_0 = 128$ ft, $(\delta v_{yr})_0 = -2$ ft/sec. The LOC curve is the localizer cross-runway position error, and FILTER is the error of the combined system using the INS and LOC as inputs, the initial covariance matrix being $P_0 = \text{diag}\{0,0,128^2 \text{ ft}^2, 2^2(\text{ft/sec})^2\}$ (the effect of range error was not investigated) and assumed localizer variance $R = \sigma_\theta^2 = 8^2\ \mu a^2$. Figure 6 shows the effects of changes in $(\sigma_y)_0 = (P_{33}{}^{(0)})^{1/2}$, $(\sigma_{vy})_0 = (P_{44}{}^{(0)})^{1/2}$, and σ_θ.

Reference 5 suggests a least-squares fit of the localizer data to obtain estimates of INS initial position and velocity errors. As explained in the Appendix, a least-squares fit may be achieved as a limiting case of a Kalman filter with large initial covariance matrix P_0. An approximation to this was accomplished, and the position errors are shown in Fig. 7.

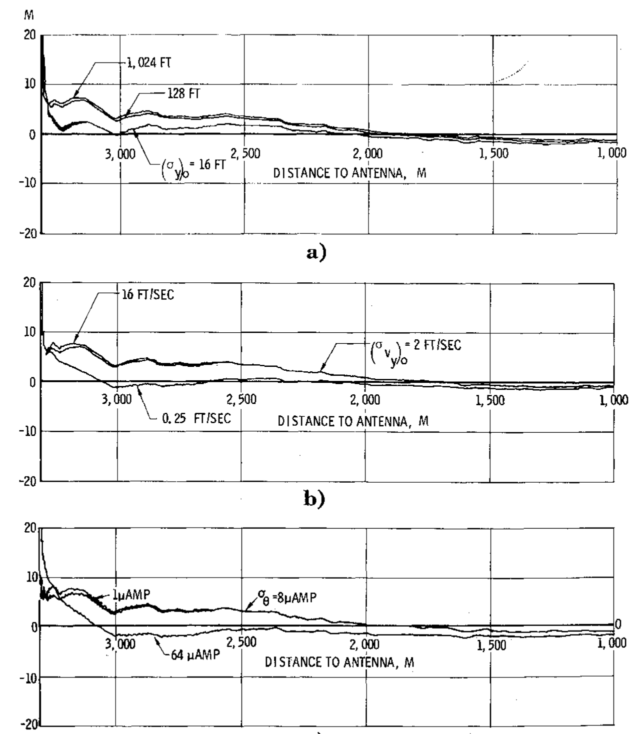

Fig. 6 a) Cross-runway position error, different initial $(P_{33})^{1/2}$; b) different initial $(P_{44})^{1/2}$; and c) different initial σ_θ.

Conclusions

Inertial data compliment ILS data available during landing approach. Tests show that it is feasible to combine inertial and ILS data in real time using the theory of optimal linear estimation, which allows simultaneous correction of ILS position errors and INS velocity errors. The resultant ILS-INS filter is relatively insensitive to initial covariance choices, an extreme choice giving a least-squares fit which also performs well. The effect of platform tilt is such that pre-correction or additional state variables will be required for poorer INS.

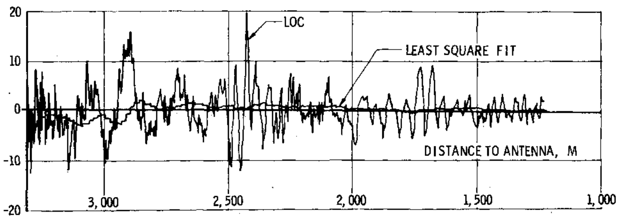

Fig. 7 Least-squares cross-runway position error, BFI runway 13R.

Appendix

Kalman Theory[6]

Given the linear system defined by a state equation

$$x_i = \Phi_{i-1}x_{i-1} + f_{i-1} + w_{i-1}, \quad \mathrm{cov}(w_i) = Q_i \tag{A1}$$

and an observation equation

$$z_i = H_i x_i + v_i, \quad \mathrm{cov}(v_i) = R_i \tag{A2}$$

The a priori estimate of the state variable before the ith observation is

$$\hat{x}_i' = \Phi_{i-1}\hat{x}_{i-1} + f_{i-1} \tag{A3}$$

with the a priori covariance matrix

$$P_i' = \Phi_{i-1}P_{i-1}\Phi_{i-1}^T + Q_{i-1} \tag{A4}$$

The Kalman gain matrix is

$$K_i = P_i'H_i(H_iP_i'H_i^T + R_i)^{-1} \tag{A5}$$

The a posteriori estimate of state variables after the ith observation is

$$\hat{x}_i = \hat{x}_i' + K_i(z_i - H_i\hat{x}_i') \tag{A6}$$

with the a posteriori covariance

$$P_i = (I - K_iH_i)P_i' \tag{A7}$$

Sequential Least Squares

Consider the case $f_i,Q_i \equiv 0,\Phi_i = \mathrm{const} = F$, and a single observation each interval whose error has constant variance, i.e., $R_i = \text{constant scalar} = r$. An estimate for the state variable at time i is obtained by solving the over-determined ($i \geq n$, n = number of state variables) system

$$\begin{aligned} H_1Fx_0 &= z_1 \\ H_2F^2x_0 &= z_2 \\ &\vdots \\ H_iF^ix_0 &= z_i \end{aligned} \quad \text{or } A_ix_0 = \begin{bmatrix} z_1 \\ z_2 \\ \cdot \\ \cdot \\ \cdot \\ z_i \end{bmatrix} \tag{A8}$$

where A_i is the ixn matrix $(H_1F,H_2F^2, \ldots, H_iF^i)^T$. The least-squares solution is

$$\hat{x}_i = F^i(A_i^TA_i)^{-1}A_i^T \begin{bmatrix} z_1 \\ \cdot \\ \cdot \\ \cdot \\ z_i \end{bmatrix} \tag{A9}$$

and the covariance of the estimate error is

$$P_i = rF^i(A_i^TA_i)^{-1}(F^T)^i \tag{A10}$$

We wish to show that the covariance satisfies the iteration (A4), (A7). We have

$$\begin{aligned} P_i &= rF^i[A_{i-1}^TA_{i-1} + (F^T)^iH_i^TH_iF^i]^{-1}(F^T)^i \\ &= rF^i[r(F^T)^{i-1}P_{i-1}^{-1}F^{i-1} + (F^T)^iH_i^TH^TF^i]^{-1}(F^T)^i \\ &= F[P_{i-1}^{-1} + (1/r)(H_iF)^T(H_iF)]^{-1}F^T \end{aligned} \tag{A11}$$

Using the formula of Sherman and Morrison,[7]

$$P_i = FP_{i-1}F^T - FP_{i-1}F^TH_i^TFP_{i-1}F^T/ (H_iFP_{i-1}F^TH_i^T + r) \tag{A12}$$

which agrees with Eqs. (A4) and (A7). A similar computation shows that the estimate (A9) may be generated sequentially by use of Eqs. (A3) and (A6). It can be shown that the exact least-squares sequence of estimates is generated in the limiting case $P_0 \to \infty I$.[6] In the tests, the approximation to least squares was not that of making P_0 large, which would cause numerical difficulties, but rather to assume an initial pair of zero localizer readings and no down-runway error, giving $x_0 \equiv 0$, and

$$P_0 = \begin{pmatrix} 0 & 0 \\ 0 & rF^2(A_2^TA_2)^{-1}(F^T)^2 \end{pmatrix} \tag{A13}$$

References

[1] Federal Aviation Administration, "Air Navigation Radio Aids," *Airman's Information Manual*, Pt. 1, Government Printing Office, Washington, D.C., Feb. 1969, pp. (1–12)–(1–15).

[2] Mercer, J. F. W., "A Quantitative Study of Instrument Approach," *Journal of the Royal Aeronautical Society*, Vol. 58, No. 518, Feb. 1954, pp. 83–108.

[3] Doniger, J., "Analytical Study of ILS Beam Characteristics," E-P Project No. AD-1091, Aug. 1962, Bendix Corp., Teterboro, N.J., pp. 8–17.

[4] Russell, W. T., "Theory of Inertial Navigation," *Inertial Guidance*, edited by G. R. Pitman, Jr., Wiley, New York, 1962, pp. 16–46.

[5] Broxmeyer, C. and Mackinnon, D., "Terminal Phase Navigation," *Navigation—Journal Institute of Navigation*, Vol. 15, No. 4, Winter 1968–9, pp. 424–430.

[6] Sorenson, H. W., "Kalman Filtering Techniques," *Advances in Control Systems*, edited by C. T. Leondes, Vol. 3, Academic Press, New York, 1966, pp. 219–292.

[7] Householder, A. S., *The Theory of Matrices in Numerical Analysis*, Blaisdell, New York, 1964, p. 123.